Eur. Phys. J. C (2023) 83:910
https://doi.org/10.1140/epjc/s10052-023-12075-9

THE EUROPEAN PHYSICAL JOURNAL C

Regular Article - Theoretical Physics

The interaction of neutrinos with phantom, quintessence, and quintum scalar fields and its effect on the formation of structures in the early universe

Muhammad Yarahmadi[a], **Amin Salehi**[b]

Department of Physics, Lorestan University, Khoramabad, Iran

Received: 2 August 2023 / Accepted: 23 September 2023 / Published online: 10 October 2023

Abstract Despite the fact that the mass of the neutrinos is so small, they are produced in such vast numbers in the early Universe that their mass induces subtle effects on cosmological observables, primarily the growth of structure and the expansion history in the Universe. We consider the models where neutrino interacts with dark energy scalar field models; phantom, quintessence, and quintom. Also, we obtained the $z_{\rm nr}$ (the redshift at which a mass of neutrino m_ν will become non-relativistic) and surveyed the effect of non-relativistic neutrinos on the structure formation. The data used in this paper are Pantheon + Analysis catalog, CMB, and BAO data. We obtained coupling constant β for neutrino and three scalar fields and found that larger β values will generally lead to larger neutrino mass in the Universe. For combination data, we found that the total mass of neutrino $\sum m_\nu < 0.1197$eV (95% confidence level (C.L.) for quintom model and $\sum m_\nu < 0.121$eV (95% confidence level (C.L.) for phantom model and $\sum m_\nu < 0.122$eV (95% confidence level (C.L.) for quintessence model. These results are in broad agreement with the results of Planck 2018 where the total neutrino mass is $\sum m_\nu < 0.12$eV (95% C.L., TT, TE, EE + lowE + lensing + BAO). Using the neutrino mass obtained from different models, we calculated $z_{\rm nr}$ and comoving wave number $k_{\rm nr}$ and showed that neutrinos played a role on the structure formation in the early Universe.

1 introduction

The model space of beyond ΛCDM cosmologies includes a range of scenarios featuring interactions between dark energy and other species [5,7,18,34,45]. Models can be constructed in which dark energy interacts with matter-energy fields. These are generally confined to couplings to cold dark matter or neutrinos. There are a number of interesting models for neutrinos acquiring a growing mass by coupling to a scalar field. These models have a scalar fields ϕ playing the role of dark energy coupled to the neutrinos in such a way that they provide a 'trigger' that causes the scalar field to leave a scaling regime and enter an inflationary regime [1,4,33,36]. If we want to explain this issue by general relativity in four dimensions, we have two ways to describe this recent cosmic expansion: one way is to modify the gravitational part of Einstein's equations [28,41], and the other being to modify the universe's contents. The simplest candidate for dark energy is the cosmological constant with equation of state parameter $\omega = -1$, which fits well with the observational evidence. If the cosmological constant is the reason for the recent cosmic acceleration, we must find a mechanism that can obtain a very small amount of it which is consistent with the observational evidence. Unfortunately, the cosmological constant has several serious problems, such as fine-tuning problem [13,31,38]. There are several candidates for dark energy such as scalar fields. A canonical scalar field is called the quintessence [35] and non-canonical scalar field is a phantom field with negative kinetic energy [16], tachyon field is derived from string theory [40], a scalar field with generalized kinetic energy called K-Essence field [6,14] and Chaplygn gas [10]. The quintessence and phantom fields in a combined model are yet another candidate for dark energy, called the quintom model [22,29,30]. As we know, in the quintessence model of dark energy, the equation of state parameter always remains greater than -1. Moreover, in the phantom model, the equation of state parameter is always less than -1. An important feature of the Quintom model is that in this model the equation of state parameter can cross the phantom boundary. Because of this, the Quintom model seems to be an inter-

[a] e-mail: Yarahmadimohammad10@gmail.com (corresponding author)
[b] e-mail: Salehi.a@lu.ac.ir

esting candidate for dark energy. While neutrinos play an important role in the early Universe cosmology, their impact on the late universe is relatively minor in ΛCDM. There are some cosmological models, however, in which neutrinos are given a central role in the late universe by means of a coupling to the dark energy. Besides, the Standard Model of Particle Physics does not explain how the neutrino masses are generated. Cosmology has helped us to come closer to explaining neutrino masses. In particular, cosmological observations are sensitive to the imprint of neutrinos on structure formation, because neutrinos suppress structure formation on small scales and slow down the growth of structure on all scales. Despite the fact that the mass of the neutrinos is so small, they are produced in such vast numbers in the early Universe that their mass induces subtle effects on cosmological observables, primarily the growth of structure and the expansion history in the Universe. Throughout the history of the Universe, neutrinos from the early Universe have evolved from a relativistic phase at very early times to a massive-particle behavior at later times [24]. Initially, neutrinos kinetic energy dominates over their rest-mass energy, and as a consequence, neutrinos can be described as massless particles fully characterized by their temperature. As the Universe cools down, the kinetic energy decreases and neutrinos undergo a transition to a non-relativistic phase with a non-negligible mass. We are interested in highlighting the role of neutrinos. In this work, we implement a cosmological model proposed by observations to put a constraint on the total neutrino mass [12,46] and the effect of neutrinos on structure formation. Scalar field plays the role of dark energy and is responsible for the accelerating expansion of the Universe.

2 The models

2.1 Phantom model

In this section, we study all three scalar fields separately. We start with the phantom dark energy. Evidence from observational data suggests that the universe is currently in a narrow band near parameter $\omega = -1$ and may be well below this value (which lies in the so-called phantom regime), an area called the Phantom Age. Phantom model is the non-canonical scalar field which is very similar to quintessence model (canonical scalar fields) except for the fact that it has negative kinetic energy. The Lagrangian of this model is:

$$L_\sigma = \frac{1}{2}\partial_\mu\sigma\,\partial^\mu\sigma - V_\sigma \tag{1}$$

where $V(\sigma) = V_0 \exp^{-\lambda\kappa\sigma}$ is a self-interacting potential in which V_0 is the potential at present, λ denotes a dimensionless parameter that determines the slope of the potential, and $\kappa = \sqrt{\frac{8\pi G}{c^4}}$. Assuming a flat space in FLRW metric filled with baryons, radiation, dark matter, dark energy and neutrinos. We start with the Friedmann equations as:

$$3H^2 = \kappa^2\left(\rho_\mathrm{b} + \rho_\mathrm{c} + \rho_\mathrm{r} + \rho_\nu - \frac{1}{2}\dot\sigma^2 + V(\sigma)\right) \tag{2}$$

where ρ_b is the baryon density, ρ_c is the cold dark matter density, ρ_r is radiation density and ρ_ν is density of neutrino.

$$2\dot H + 3H^2 = \kappa^2(-\omega_\mathrm{b}\rho_\mathrm{b} - \omega_\mathrm{c}\rho_\mathrm{c} + \omega_\mathrm{r}\rho_\mathrm{r} - \omega_\nu\rho_\nu + \frac{1}{2}\dot\sigma^2 + V(\sigma)) \tag{3}$$

The energy density conservation equations are:

$$\dot\rho_\sigma + 3H\rho_\sigma(1+\omega_\sigma) = -\beta\rho_\nu(1-3\omega_\nu)\dot\sigma \tag{4}$$

The action of neutrino-scalar field interaction resulting from [8] can also be considered in the context of the coupled scalar field model [5,44,45]. By employing the Fermi-Dirac distribution for neutrinos whose masses $m_\nu(\sigma)$ are σ dependent and also in thermal equilibrium with temperature $T(\nu)$, one obtains

$$\rho_\nu = \frac{T^4_{(\nu)}}{\pi^2}\int_0^\infty \frac{dx x^2\sqrt{x^2+\xi^2}}{e^x+1} \tag{5}$$

$$p_\nu = \frac{T^4_{(\nu)}}{3\pi^2}\int_0^\infty \frac{dx x^4}{e^x+1\sqrt{x^2+\xi^2}} \tag{6}$$

where $\xi = \frac{m_\nu(\sigma)}{T_{(\nu)}}$. By using above equation one finds

$$\dot\rho_\nu + 3H(\rho_\nu + p_\nu) = \beta\dot\sigma(\rho_\nu - 3p_\nu) \tag{7}$$

Also, [11] used the same way to drive Eq. 7.

$$\dot\rho_\nu + 3H\rho_\nu(1+\omega_\nu) = \beta\rho_\nu(1-3\omega_\nu)\dot\sigma \tag{8}$$

Note that if $\omega_\nu = \frac{1}{3}$, the coupling vanishes making neutrinos non-interacting particles.

$$\dot\rho_\mathrm{c} + 3H\rho_\mathrm{c} = -\alpha\rho_\mathrm{c}\dot\sigma \tag{9}$$

$$\dot\rho_\mathrm{b} + 3H\rho_\mathrm{b} = 0 \tag{10}$$

$$\dot\rho_\mathrm{r} + 4H\rho_\mathrm{r} = 0 \tag{11}$$

respectively. Where the coupling parameter β can, in general, be some function of σ. The coupling plays a role only when the neutrinos are non-relativistic, since relativistic neutrinos have $P_\upsilon \approx \frac{\rho_\upsilon}{3}$; therefore, the right-hand sides of Eqs. (3.4) and (3.7) are both negligible such that the standard, uncoupled conservation equations are recovered. Since dark energy is modeled as a scalar field σ its energy density and pressure are given by

$$\rho_\sigma = \frac{-1}{2}\dot\sigma^2 + V(\sigma), \quad p_\sigma = \frac{-1}{2}\dot\sigma^2 - V(\sigma) \tag{12}$$

where $V(\sigma)$ denotes the potential of the scalar field. In this paper, we consider the coupling between dark energy and

neutrino as the following evolution equation. In addition, from the resulting equations of the scalar field:

$$\ddot{\sigma} = -\lambda V(\sigma) - \frac{3}{2}H\dot{\sigma}(1+\omega_\sigma) - \frac{3HV}{\dot{\sigma}}(1+\omega_\phi) + \beta\rho_\nu(1-3\omega_\nu) \tag{13}$$

where as before $\dot{a}$ means differentiation with respect to the coordinate time t. The EoS of the scalar field is now given by:

$$\omega_\sigma = \frac{\frac{1}{2}\dot{\sigma}^2 + V(\sigma)}{\frac{1}{2}\dot{\sigma}^2 - V(\sigma)} \tag{14}$$

The above equations are a nonlinear set of second-order differential equations that can only be solved analytically for certain cases. To simplify the equations, we can introduce a number of new variables to turn the second-order differential equations into a set of first-order equations. There are several reasons for this, including:

1. Systems of the first order for the numerical solution are very simple and convenient. On the other hand, it allows us to study the behavior of the system in phase space.
2. In the numerical solution of first-order equations, unlike high-order equations, which require more than one condition for each equation, only one initial condition is required.
3. Most importantly, the first-order dynamics can be described on the phase space and it is possible to check the stability of the system.

If we considered the standard model, the right side of the equation would be zero, and the neutrinos effectively uncoupled. We consider an exponential potential $V(\sigma) = V_0\, e^{-\lambda k\sigma}$, where λ is a dimensionless parameter that determines the slope of the potential. The motivation for choosing these functions have been investigated in [45]. Furthermore, we define $\omega = \frac{P_\nu}{\rho_\nu}$. In order to simplify the field equations, we introduce the following new variables,

$$\begin{aligned} &\xi_1 = \frac{\kappa^2\rho_\mathrm{b}}{3H^2} \quad \xi_2 = \frac{\kappa^2\rho_\nu}{3H^2} \quad \xi_3 = \frac{\kappa^2\rho_\mathrm{r}}{3H^2} \\ &\xi_4 = \frac{\kappa^2\rho_c}{3H^2} \quad \xi_5 = -\frac{\kappa\dot{\sigma}}{\sqrt{6}H} \quad \xi_6 = \frac{\kappa^2 V(\sigma)}{3H^2} \end{aligned} \tag{15}$$

In term of new variable the Friedmann equations (2) puts a constraint on new variables as

$$\xi_6 = 1 - \xi_1 - \xi_2 - \xi_3 - \xi_4 + \xi_5^2 \tag{16}$$

Therefore, the equations are simplified as follows:

$$\frac{d\xi_1}{dN} = -3\xi_1 - 2\xi_1\frac{\dot{H}}{H^2} \tag{17}$$

$$\frac{d\xi_2}{dN} = -\xi_2\left(3(1+\omega_\nu) + \sqrt{6}\xi_5\beta(1-3\omega_\nu)\right) - 2\xi_2\frac{\dot{H}}{H^2} \tag{18}$$

$$\frac{d\xi_3}{dN} = -4\xi_3 - 2\xi_3\frac{\dot{H}}{H^2} \tag{19}$$

$$\frac{d\xi_4}{dN} = -\xi_4\left(3 - \sqrt{6}\xi_5\alpha + 2\frac{\dot{H}}{H^2}\right) \tag{20}$$

$$\frac{d\xi_5}{dN} = \frac{3\lambda\xi_6}{\sqrt{6}} - \frac{3\beta\xi_2(1-3\omega_\nu)}{\sqrt{6}} + \frac{9\alpha}{\sqrt{6}}\xi_4 + 3\xi_5 - \xi_5\frac{\dot{H}}{H^2} \tag{21}$$

Where, $N = \ln a$. In term of the new dynamical variable, we also have,

$$\frac{\dot{H}}{H^2} = \frac{1}{2}\left(-3 - \xi_3 - 3\omega_\nu\xi_2 + 3\xi_5^2 + 3\xi_6\right) \tag{22}$$

The above parameter is very important, since essential cosmological parameters such as deceleration parameters q and effective equation of state (EoS) w_eff can be expressed in terms of this parameter as $q = -1 - \frac{\dot{H}}{H^2}$ and $w_\mathrm{eff} = -1 - \frac{2}{3}\frac{\dot{H}}{H^2}$. It is also used in calculating the luminosity distance. The equation related to the luminosity distance is coupled by these parameters with the equations of the system. We used the same approach with [39].

When neutrinos are non-relativistic, one needs to limit the value of N_eff accordingly. Also, the matter density must contain the neutrino contribution.

$$\Omega_\mathrm{m} = \Omega_\nu + \Omega_\mathrm{b} + \Omega_\mathrm{c} \tag{23}$$

where Ω_ν is related to the sum of neutrino masses as

$$\Omega_\nu = \frac{\sum m_\nu}{94h^2} \tag{24}$$

In addition to photons, neutrinos and other relativistic degrees of freedom make up the total relativistic energy density in the early universe. N_eff parameter is used to show the effective number of relativistic species. Its standard value of 3.046 corresponds to the case of three generations of N_eff neutrinos with no additional dark radiation. Therefore, the total radiation energy density in the Universe is calculated by

$$\rho_\mathrm{r} = \rho_\gamma\left(1 + \frac{7}{8}\left(\frac{4}{11}\right)^{\frac{4}{3}}N_\mathrm{eff}\right) \tag{25}$$

where ρ_γ is the energy density of photons. This value of N_eff indicates that if it is higher than 3.046, there is a dark radiation that is other than three generations of neutrinos.

The expected linear correlation between $\Omega_\mathrm{m}h^2$ and N_eff given by

$$N_\mathrm{eff} = 3.04 + 7.44\left(\frac{\Omega_\mathrm{m}h^2}{0.1308}\frac{3139}{1+z_\mathrm{eq}} - 1\right). \tag{26}$$

2.2 Quintessence model

Quintessence is described as a canonical scalar field that is minimally coupled to gravity. Compared to other models of scalar fields such as phantoms, the simplest scenario is the scalar field. A variable slow field along with a potential can accelerate the universe. This mechanism is similar to slow inflation in the early universe; the difference is that non-relative matter (dark matter and baryon) cannot be ignored to properly discuss dark energy dynamics. The action which will then represent our physical system is:

$$S = \int d^4x\sqrt{-g}\left(\frac{R}{2\kappa^2} + L_m + L_\phi\right) \tag{27}$$

where L_ϕ is the canonical Lagrangian of a scalar field ϕ uniquely given by

$$L_\phi = -\frac{1}{2}\partial_\mu\phi\partial^\mu\phi - V(\phi) \tag{28}$$

Now, we analyze the quintessence model. We start with Friedmann and acceleration equation [32,35,45,48]:

$$3H^2 = \kappa^2\left(\rho_\mathrm{b} + \rho_\mathrm{c} + \rho_\mathrm{r} + \rho_\nu + \frac{1}{2}\dot{\phi}^2 + V(\phi)\right) \tag{29}$$

$$2\dot{H} + 3H^2 = -\kappa^2(\omega_\mathrm{b}\rho_\mathrm{b} + \omega_\mathrm{c}\rho_\mathrm{c} + \omega_\mathrm{r}\rho_\mathrm{r} + \omega_\nu\rho_\nu + \frac{1}{2}\dot{\phi}^2 - V(\phi)). \tag{30}$$

The evolution equations for their energy densities are:

$$\dot{\rho}_\phi + 3H\rho_\phi(1+\omega_\phi) = -\beta\rho_\nu(1-3\omega_\nu)\dot{\phi} \tag{31}$$

$$\dot{\rho}_\nu + 3H\rho_\nu(1+\omega_\nu) = \beta\rho_\nu(1-3\omega_\nu)\dot{\phi} \tag{32}$$

while the Klein–Gordon equation is:

$$\ddot{\phi} = \lambda V(\phi) - \frac{3}{2}H\dot{\phi}(1+\omega_\phi) - \frac{3HV}{\dot{\phi}}(1+\omega_\phi) - \beta\rho_\nu(1-3\omega_\nu) \tag{33}$$

We can define the energy density and pressure of the scalar field as follows:

$$\rho_\phi = \frac{1}{2}\dot{\phi}^2 + V(\phi) \tag{34}$$

$$p_\phi = \frac{1}{2}\dot{\phi}^2 - V(\phi). \tag{35}$$

The resulting equation of state is as follows:

$$\omega_\phi = \frac{\frac{1}{2}\dot{\phi}^2 - V(\phi)}{\frac{1}{2}\dot{\phi}^2 + V(\phi)} \tag{36}$$

where ω_ϕ is a dynamically evolving parameter which can take values in the range $[-1, 1]$. We rewrite the cosmological equations (3.24), (3.25) and (3.26) into an autonomous system of equations.

$$\chi_1 = \frac{\kappa^2\rho_\mathrm{b}}{3H^2} \quad \chi_2 = \frac{\kappa^2\rho_\nu}{3H^2} \quad \chi_3 = \frac{\kappa^2\rho_\mathrm{r}}{3H^2}$$
$$\chi_4 = \frac{\kappa^2\rho_c}{3H^2} \quad \chi_5 = -\frac{\kappa\dot{\sigma}}{\sqrt{6}H} \quad \chi_6 = \frac{\kappa^2V(\phi)}{3H^2} \tag{37}$$

we can derive the following dynamical system:

$$\chi_6 = 1 - \chi_1 - \chi_2 - \chi_3 - \chi_4 + \chi_5^2 \tag{38}$$

Therefore, the equations are simplified as follows:

$$\frac{d\chi_1}{dN} = -3\chi_1 - 2\chi_1\frac{\dot{H}}{H^2} \tag{39}$$

$$\frac{d\chi_2}{dN} = -\chi_2\left(3(1+\omega_\nu) - \sqrt{6}\chi_5\beta(1-3\omega_\nu)\right) - 2\chi_2\frac{\dot{H}}{H^2} \tag{40}$$

$$\frac{d\chi_3}{dN} = -4\chi_3 - 2\chi_3\frac{\dot{H}}{H^2} \tag{41}$$

$$\frac{d\chi_4}{dN} = -\chi_4\left(3 + \sqrt{6}\chi_5\alpha + 2\frac{\dot{H}}{H^2}\right) \tag{42}$$

$$\frac{d\chi_5}{dN} = \frac{3\lambda\chi_6}{\sqrt{6}} - \frac{3\beta\chi_2(1-3\omega_\nu)}{\sqrt{6}} + \frac{9\alpha}{\sqrt{6}}\chi_4 - 3\chi_5 - \chi_5\frac{\dot{H}}{H^2} \tag{43}$$

where, $N = \ln a$. In terms of the new dynamical variables, we also have,

$$\frac{\dot{H}}{H^2} = \frac{1}{2}\left(-3 - \chi_3 - 3\omega_\nu\chi_2 - 3\chi_5^2 + 3\chi_6\right) \tag{44}$$

Using the relationships mentioned to estimate the mass of neutrinos and N_eff in the previous section, we have:

2.3 Quintom model

In the previous section we found that the equation of state in the quintessence model must satisfy $\omega_\mathrm{de} \geq -1$, we also saw that in the phantom scalar field, EoS is limited to $\omega_\mathrm{de} < -1$. There seems to be no way to cross the phantom barrier (i.e. the cosmological constant $\omega_\mathrm{de} = -1$) using a scalar field. To cross this barrier, the Quintom model is used, which allows such a passage. This dark energy scenario causes the EoS to be larger than -1 and less than -1, which satisfies current observations. The simplest model is represented by a quantum Lagrangian consisting of two scalar fields, a canonical field ϕ (quintessence) and a phantom field σ:

$$L_{quintom} = -\frac{1}{2}\partial_\mu\phi\partial^\mu\phi + \frac{1}{2}\partial_\mu\sigma\partial^\mu\sigma - V(\sigma,\phi) \tag{45}$$

where $V(\phi,\sigma)$ is

$$V(\sigma,\phi) = V_0 \exp^{-\lambda_\phi\kappa\phi-\lambda_\sigma\kappa\sigma} \tag{46}$$

a general potential for both scalar fields and ϕ and σ represents the quintessence and phantom fields, respectively. In above equation λ_ϕ and λ_σ are constant values. The kinetic energy sign is positive for the quintessence model and negative for the phantom model. The cosmological equations are given by the Friedmann and acceleration equations [22,47]:

$$3H^2 = \kappa^2\left(\rho_b + \rho_c + \rho_r + \rho_\nu + \frac{1}{2}\dot\phi^2 + V(\sigma,\phi) - \frac{1}{2}\dot\sigma^2\right) \tag{47}$$

$$2\dot H + 3H^2 = -\kappa^2(\omega_b\rho_b + \omega_c\rho_c + \omega_r\rho_r + \omega_\nu\rho_\nu + \frac{1}{2}\dot\phi^2 + V(\sigma,\phi) - \frac{1}{2}\dot\sigma^2) \tag{48}$$

The energy density conservation equations are:

$$\dot\rho_(\sigma,\phi) + 3H\rho_{(\sigma,\phi)}(1+\omega_{(\sigma,\phi)}) = -\beta\rho_\nu(1-3\omega_\nu)(\dot\sigma+\dot\phi) \tag{49}$$

$$\dot\rho_\nu + 3H\rho_\nu(1+\omega_\nu) = \beta\rho_\nu(1-3\omega_\nu)(\dot\sigma+\dot\phi) \tag{50}$$

and by the Klein–Gordon equations we have

$$\ddot\phi = \lambda_\phi V - \frac{3}{2}H\dot\phi(1+\omega_\phi) - \frac{3HV}{\dot\phi}(1+\omega_\phi) - \beta\rho_\nu(1-3\omega_\nu) \tag{51}$$

$$\ddot\sigma = -\lambda_\sigma V - \frac{3}{2}H\dot\sigma(1+\omega_\sigma) + \frac{3HV}{\dot\sigma}(1+\omega_\sigma) + \beta\rho_\nu(1-3\omega_\nu). \tag{52}$$

To recreate them in a dynamic system, we define the EN variables

$$\eta_1 = \frac{\kappa^2\rho_b}{3H^2} \quad \eta_2 = \frac{\kappa^2\rho_c}{3H^2} \quad \eta_3 = \frac{\kappa^2\rho_r}{3H^2} \quad \eta_4 = \frac{\kappa^2\rho_\nu}{3H^2}$$
$$\eta_5 = \frac{\kappa\dot\phi}{\sqrt{6}H} \quad \eta_6 = -\frac{\kappa\dot\sigma}{\sqrt{6}H} \quad \eta_7 = \frac{\kappa^2V(\sigma,\phi)}{3H^2}. \tag{53}$$

To find the dynamics of the system governing cosmic evolution, we follow the same method we used for the previous two models.

$$\frac{d\eta_1}{dN} = -3\eta_1 - 2\eta_1\frac{\dot H}{H^2} \tag{54}$$

$$\frac{d\eta_3}{dN} = -4\eta_3 - 2\eta_3\frac{\dot H}{H^2} \tag{55}$$

$$\frac{d\eta_4}{dN} = -3\eta_4(1+\omega_\nu) - \beta\sqrt{6}(1-3\omega_\nu)\eta_4\eta_6 + \beta\sqrt{6}(1-3\omega_\nu)\eta_4\eta_5 - 2\eta_4\frac{\dot H}{H^2} \tag{56}$$

$$\frac{d\eta_5}{dN} = \frac{3\lambda_\phi}{\sqrt{6}}\eta_7 - \frac{3}{2}(1+\omega_\phi)\eta_5 - \frac{3}{2}(1+\omega_\phi)\frac{\eta_7}{\eta_5} - \frac{3\beta}{\sqrt{6}}(1-3\omega_\nu)\eta_4 - \eta_5\frac{\dot H}{H^2} \tag{57}$$

$$\frac{d\eta_6}{dN} = \frac{3\lambda_\sigma}{\sqrt{6}}\eta_7 - \frac{3}{2}(1+\omega_\sigma)\eta_6 - \frac{3}{2}(1+\omega_\phi)\frac{\eta_7}{\eta_6} - \frac{3\beta}{\sqrt{6}}(1-3\omega_\nu)\eta_4 + \eta_6\frac{\dot H}{H^2} \tag{58}$$

$$\frac{d\eta_7}{dN} = \eta_7\left(\sqrt{6}\lambda_\sigma\eta_6 - \sqrt{6}\lambda_\phi\eta_5 - 2\frac{\dot H}{H^2}\right) \tag{59}$$

and the Friedmann constraint is

$$\eta_2 = 1 - \eta_1 - \eta_3 - \eta_4 - \eta_5^2 + \eta_6^2 - \eta_7 \tag{60}$$

holds.

3 Numerical analysis

Connecting theory to data is an integral part of the scientific process. Generally a cosmological observable refers to a specific phenomenon or class of objects which can be used to measure some key properties of cosmology, most commonly the clustering of matter at some particular epoch and within some set of length scales. These observations allow us to compare theoretical predictions to data, and thereby constraint properties of the cosmological model. All observational data used in this paper are:

- Pantheon catalog: [42] compiled the Pantheon sample consisting 1701 SNe Ia covering the redshift range $0.001 < z < 2.3$.
- CMB data: We used the latest large-scale cosmic microwave background (CMB) temperature and polarization angular power spectra from the final release of Planck 2018 plikTTTEEE + lowl + lowE [2].
- BAO data: We also used the various measurements of the Baryon Acoustic Oscillations (BAO) from different galaxy surveys [2], i.e. 6dFGS.(2011) [9], SDSS-MGS [37], and BOSS DR12 (2017) [4].

To analyze the data and extract the constraints on these cosmological parameters, we used our modified version of the publicly available Monte Carlo Markov Chain package CosmoMC [25]. This is equipped with a convergence diagnostic based on the Gelman and Rubin statistic [21], assuming $R - 1 < 0.02$, and implements an efficient sampling of the pos- terior distribution using the fast/slow parameter decorrelations [26]. CosmoMC includes support for the 2018 Planck data release [2]. We also used the Akaike Information Criteria (AIC)

$$AIC = \chi^2_{\min} + 2k \tag{61}$$

In these equations $\chi^2_{\rm min}$ is the minimum value of χ^2, k is the number of parameters of the given model. AIC provides means to compare models with different numbers of parameters; they penalize models with a higher k in favor of those with a lower k, in effect enforcing Occam's Razor in the model selection process.

We put constraints on the following cosmological parameters: the baryon energy density $\Omega_b h^2$, the cold dark matter energy density $\Omega_c h^2$, ($\sum m_\nu$ total mass of neutrino, $N_{\rm eff}$ effective number of relativistic species, H_0 Hubble constant, λ a dimensionless parameter that determines the slope of the potential.

Phantom Model:

In what follows, we put constraint on the total mass of neutrino by analyzing of Pantheon and CMB and BAO data. We first survey the results of the CMB + Pantheon data and then investigate the results of CMB + BAO, and finally survey the total results of these two parts. The results for the cosmological parameters are shown in Table 1. Figure 1 also shows the parametric space at 68% CL and 95% CL for some selected parameters for the different observational data sets.

From the analysis of the CMB + BAO data and, for phantom we find that $\sum m_\nu < 0.168$eV (95% CL.) and using CMB+Pantheon+ we find $\sum m_\nu < 0.22$eV (95% CL.) and for combination of full data(CMB+BAO+Pantheon+) we find $\sum m_\nu < 0.121$eV (95% CL.) (Fig. 2). For results from combined data (Pantheon + CMB + BAO), we consider multivariate joint Gaussian likelihood given by

$$\mathcal{L}_{\rm Joint} \propto \exp\left(\frac{-\chi^2_{\rm Joint}}{2}\right), \tag{62}$$

where the joint chi-squared function of all the datasets reads

$$\chi^2_{\rm Joint} = \chi^2_{\rm BAO} + \chi^2_{\rm CMB} + \chi^2_{\rm Pantheon}. \tag{63}$$

Quintessence Model:

From the analysis of the CMB + BAO data, for quintessence we find that $\sum m_\nu < 0.162$eV (95% CL.) and using CMB + Pantheon+ we find $\sum m_\nu < 0.224$eV (95% CL.) and for combination of full data (CMB + BAO + Pantheon+) we find $\sum m_\nu < 0.122$eV (95% CL.) (Figs. 3, 4, Table 2).

Quintom Model:

For CMB + BAO data, we find that $\sum m_\nu < 0.128$eV (95%CL.) and using CMB + Pantheon+ we find $\sum m_\nu < 0.2$eV (95% CL.) and for combination of full data (CMB + BAO + Pantheon+) we find $\sum m_\nu < 0.1197$eV (95% CL.) (Figs. 5, 6).

This result is close to results of [2] TT,TE,EE + lowE + lensing + BAO with $\sum m_\nu < 0.12$eV at 95% CL and case TT,TE,EE + lowE + BAO with $\sum m_\nu < 0.13$ eV at 95% CL

Table 1 Observational constraints at (95% CL.) on main and derived parameters of the $\sum m_\nu$ scenario. The parameter H_0 is in the units of km/s/Mpc, whereas $\sum m_\nu$ reported in the (95% CL.), is in the units of eV (Phantom model)

Dataset	$\Omega_b h^2$	$\Omega_c h^2$	H_0	Ω_m	$\Omega_m h^2$	$\sum m_\nu$	β	λ	$N_{\rm eff}$
CMB + BAO	0.02233 ± 0.00019	0.1184 ± 0.0034	69.91 ± 1.4	0.3087 ± 0.0071	$0.1414^{+0.0024}_{-0.0021}$	< 0.168	$0.173^{+0.37}_{-0.25}$	1.01 ± 0.4	2.98 ± 0.17
CMB + Pantheon	$0.02238 \pm 0.00018 \pm 0.00019$	0.1181 ± 0.0029	71.05 ± 1	0.3017 ± 0.0071	0.1272 ± 0.004	< 0.22	0.171 ± 0.29	$0.72^{+0.2}_{-0.3}$	3.02 ± 0.20
CMB + BAO + Pantheon	0.02237 ± 0.00018	0.1187 ± 0.0025	70.4 ± 2	0.3111 ± 0.0071	0.1263 ± 0.002	< 0.121	0.229 ± 0.42	$0.8^{+0.5}_{-0.5}$	3.00 ± 0.15

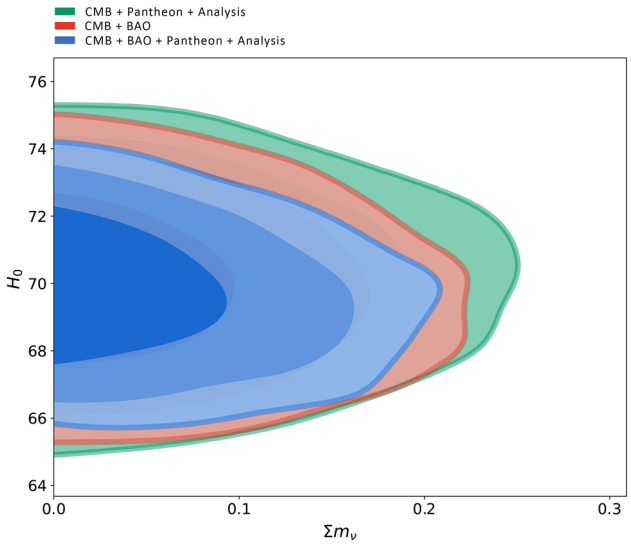

Fig. 1 The constraints at the (95% CL.) two-dimensional contours for $\sum m_\nu$ for phantom model

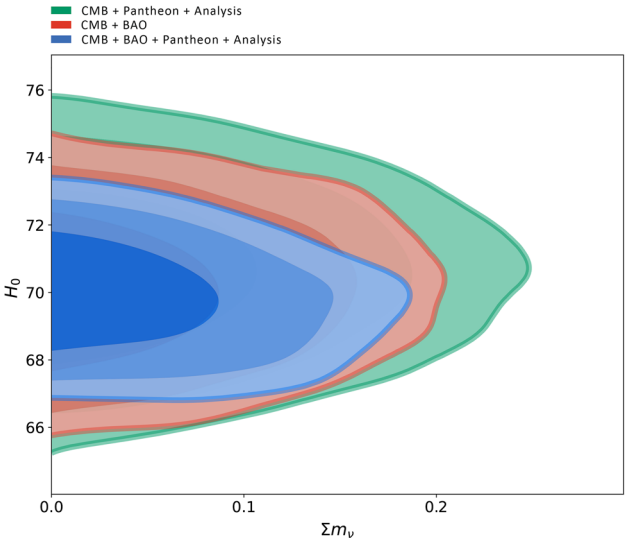

Fig. 3 The constraints at the (95% CL.) two-dimensional contours for $\sum m_\nu$ in quintessence model

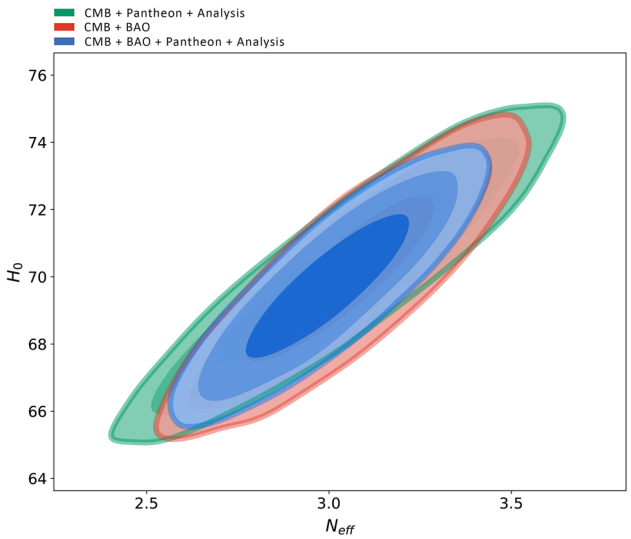

Fig. 2 The constraints at the (68% CL.) two-dimensional contours for $N_{\rm eff}$ in phantom model

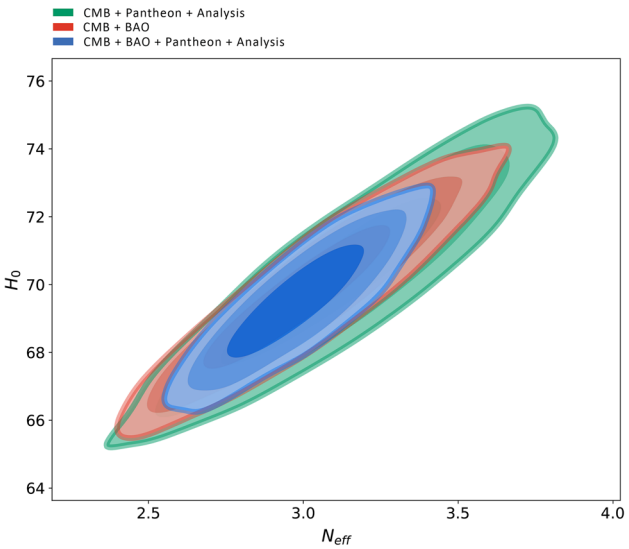

Fig. 4 The constraints at the (68% CL.) two-dimensional contours for $N_{\rm eff}$ in quintessence model

in three models. Other parameters are shown in Tables 3, 4, 5.

Moreover, we obtain the Δ(AIC) between ΛCDM and each model (Figs. 7, 8, 9, 10).

- The value of Δ(AIC) between the phantom model and ΛCDM is 0.299.
- The value of Δ(AIC) between the Quintessence model and ΛCDM is 1.406.
- The value of Δ(AIC) between the Quintom model and ΛCDM is 6.021.

In the following, we estimate the Neutrinos transition from relativistic to non-relativistic at redshift $z_{\rm nr}$ for all three models. Neutrinos decouple from the primordial plasma in a Fermi-Dirac distribution:

$$f(p_\nu, T_\nu) = \left[\exp\left(\frac{p_\nu}{T_\nu}\right) + 1\right]^{-1} \tag{64}$$

with temperature T_ν. The average momentum is related to the temperature by $\langle p_\nu \rangle = 3.15 T_\nu$. Massive neutrinos become non-relativistic when p_ν falls below their rest mass. The temperature of the CNB is related to the temperature of the CMB

Table 2 Observational constraints at (95% CL.) on main and derived parameters of the $\sum m_\nu$ scenario. The parameter H_0 is in the units of km/s/Mpc, whereas $\sum m_\nu$ reported in the 95% CL, is in the units of eV (Quintessence Model)

Dataset	$\Omega_b h^2$	$\Omega_c h^2$	H_0	Ω_m	$\Omega_m h^2$	$\sum m_\nu$	β	λ	N_{eff}
CMB + BAO	0.02231 ± 0.00019	$0.1181^{+0.0030}_{-0.0034}$	69.88 ± 1.8	0.3092 ± 0.0084	$0.127^{+0.0028}_{-0.0027}$	< 0.162	$0.186^{+0.31}_{-0.36}$	0.22 ± 0.3	2.99 ± 0.20
CMB + Pantheon	0.02225 ± 0.00024	0.1200 ± 0.0037	70.54 ± 1.4	0.325 ± 0.01	0.1263 ± 0.004	< 0.324	0.141 ± 0.29	$0.714^{+0.4}_{-0.35}$	3.11 ± 0.23
CMB + BAO + Pantheon	0.02236 ± 0.00017	0.1183 ± 0.0024	70.75 ± 1.23	0.3108 ± 0.0069	$0.124^{+0.006}_{-0.005}$	< 0.122	$0.632^{+0.7}_{-0.7}$	$8.1^{+0.74}_{-0.63}$	2.98 ± 0.14

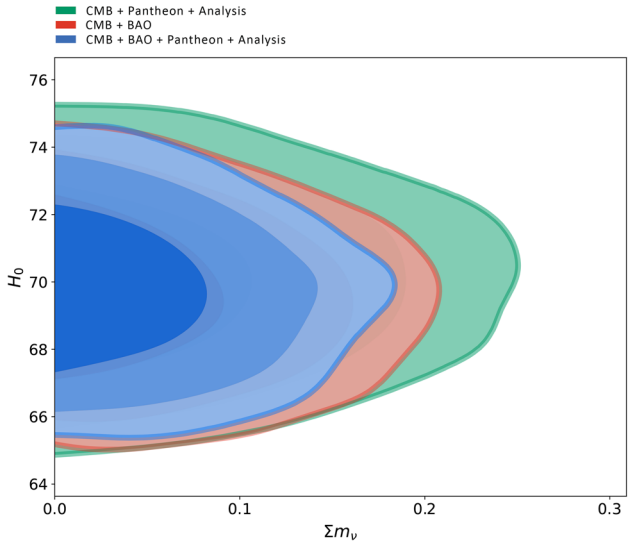

Fig. 5 The constraints at the (95% CL.) two-dimensional contours for $\sum m_\nu$ in quintom model

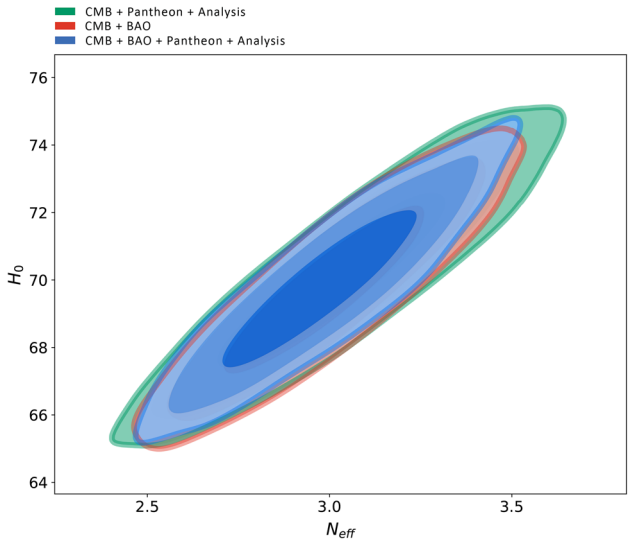

Fig. 6 The constraints at the (68% CL.) two-dimensional contours for $N_{\rm eff}$ in quintom model

by:

$$T_\nu{}^0 = \left(\frac{4}{11}\right)^{\frac{1}{3}} T^0{}_{CMB}. \tag{65}$$

Using a CMB temperature of 2.725 K and given that in general $T(z) = T_0(1+z)$, we can then estimate the redshift at which a neutrino of mass m_ν will become non-relativistic as:

$$z_{nr} = \left(\frac{m_\nu}{5.28 \times 10^{-4} ev}\right) - 1. \tag{66}$$

According to the above equation and the values obtained for the neutrino mass in all three models, we will calculate

Table 3 Observational constraints at (95% CL.) on main and derived parameters of the $\sum m_\nu$ scenario. The parameter H_0 is in the units of km/s/Mpc, whereas $\sum m_\nu$ reported in the (95% CL.), is in the units of (eV) (Quintom)

Dataset	$\Omega_b h^2$	$\Omega_c h^2$	H_0	Ω_m	$\sum m_\nu$	β	λ_σ	λ_ϕ	N_{eff}
CMB + BAO	0.02238 ± 0.00019	0.1185 ± 0.0030	69.95 ± 1.73	0.3109 ± 0.0073	< 0.128	0.151 ± 0.25	-2.75 ± 0.5	2.83 ± 0.07	2.99 ± 0.18
CMB + Pantheon	0.02233 ± 0.00017	0.1181 ± 0.0034	70.92 ± 1.55	0.3087 ± 0.0071	< 0.2	0.164 ± 0.4	-2.9 ± 0.05	$1.91^{+0.011}_{-0.017}$	$2.97^{+0.32}_{-0.35}$
CMB + BAO + Pantheon	0.02238 ± 0.00012	0.1180 ± 0.0019	71.03 ± 1.1	0.3099 ± 0.0054	< 0.119	0.236 ± 0.4	$-2.63^{+0.05}_{-0.03}$	$2.6^{+0.014}_{-0.028}$	2.98 ± 0.17

Table 4 Mean values of free parameters of various models with 1σ error bar for combinations data

Models	Ω_ϕ	Ω_m	Ω_Λ	Ω_σ	β	Ω_ν	H_0	AIC
ΛCDM	–	0.311 ± 0.15	0.678 ± 0.17	–	–	–	68.9 ± 1.3	3599.172
Phantom	–	0.309 ± 0.0055	–	0.61 ± 0.075	0.229 ± 0.43	0.0012 ± 0.0009	70.04 ± 1.42	3598.873
Quintessence	0.64 ± 0.04	0.3108 ± 0.0069	–	–	0.63 ± 0.7	0.003 ± 0.0014	70.25 ± 1.23	3597.766
Quintom	0.08 ± 0.022	0.3111 ± 0.0071	–	0.62 ± 0.064	0.236 ± 0.4	0.0026 ± 0.0011	71.03 ± 1.1	3593.151

the the redshift at which a neutrino of mass m_ν will become non-relativistic (z_{nr}):

- For the phantom model (combination data) we obtained $z_{\rm nr} = 228.166.$s
- For the quintessence model (combination data) we obtained $z_{\rm nr} = 230.060$.
- For the quintom model (combination data) we obtained $z_{\rm nr} = 225.704$.

Now we can discuss the effect of neutrinos in the structures formation in the early universe. An important quantity in the context of structure formation is the Jeans length, which traditionally refers to the length scale below which gravitational collapse is counteracted by pressure forces:

$$k_J(t) = \left(\frac{4\pi G\bar{\rho}(t)a^2(t)}{c_s^2(t)}\right)^{\frac{1}{2}}. \tag{67}$$

Here G is Newton's gravitational constant, $\bar{\rho}(t)$ is the mean density of the fluid, and $c_s^2(t)$ is the squared speed of sound in the fluid. Although massive neutrinos are effectively collisionless particles, replacing $c_s^2(t)$ with the thermal velocity, ${v_{\rm th}}^2(t)$ defines a free-streaming scale, below which massive neutrinos do not cluster. Using the Friedman equation, we can then write this as

$$k_{FS}(t) = \sqrt{\frac{3}{2}}\frac{v_{\rm th}(t)}{H(t)}. \tag{68}$$

For relativistic neutrinos, where $v = c$, this scale is simply the Hubble radius. For non-relativistic neutrinos, their thermal velocity evolves as

$$\begin{aligned} v_{th} &= \frac{\langle p_\nu\rangle}{m_\nu} \approx \frac{3T_\nu}{m_\nu} = \frac{3T_\nu^0}{m_\nu}(1+z) \\ &\approx 150(1+z)\left(\frac{1ev}{m_\nu}\right) kms^{-1}. \end{aligned} \tag{69}$$

We can then write an instantaneous free-streaming scale as a function of neutrino mass:

$$k_{FS}(z) = 0.82\frac{\sqrt{\Omega_\Lambda + \Omega_{\rm m}(1+z)^3}}{(1+z)^2}\left(\frac{m_\nu}{1ev}\right) h\ Mpc^{-1} \tag{70}$$

This scale reaches a minimum wavenumber at $z_{\rm nr}$, so we can define a minimum free- streaming wavenumber:

$$k_{\rm nr} \approx 0.018{\Omega_{\rm m}}^{\frac{1}{2}}\left(\frac{m_\nu}{1ev}\right)^{\frac{1}{2}} h\ Mpc^{-1}. \tag{71}$$

On scales larger than this, neutrinos effectively evolve like an additional component of the dark matter. On smaller scales, neutrino free-streaming means the neutrinos do not cluster, suppressing the matter power spectrum on these scales. In linear theory, this suppression can be analytically calculated to be $(1 - 8f_\nu)$ with respect to the massless neutrino case on scales $k \gg k_{\rm nr}$, where $f_\nu = \frac{\Omega_\nu}{\Omega_{\rm m}}$. In turn, free-streaming (non-clustering) neutrinos slow down the growth of gravitational potential wells on scales $\lambda \ll \lambda_{\rm FS}$ or wave numbers $k \gg k_{\rm FS}$. What is more, massive neutrinos make up a fraction of the dark matter, however, due to their large thermal velocities, cluster significantly less than cold dark matter (CDM) on small scales. According to the values obtained for the mass of neutrinos in these three models(quintessence, phantom, and quintom), we will estimate the co-moving wave number.

- For the phantom model(combination data) we obtained the non-relativistic neutrino wavenumber $k_{\rm nr} = 0.0.000243{\rm Mp}c^{-1}$.
- For the quintessence model(combination data) we obtained the non-relativistic neutrino wavenumber $k_{\rm nr} = 0.000248{\rm Mp}c^{-1}$.
- For the quintom model(combination data) we obtained the non-relativistic neutrino wavenumber $k_{\rm nr} = 0.000245{\rm Mp}c^{-1}$.

These results are in general agreement with [15,27].

In addition to the above scenario, we consider the scenario when $\sum m_\nu$ equals to the minimum value in each hierarchy and the lightest neutrino is massless (Fig. 11).

The results of oscillation experiments [3,17,20,23] lead to two possible orderings of the neutrino mass eigenstates. In Fig. 10: on the left, the normal hierarchy has $m1 < m2 < m3$, and on the right the inverted hierarchy has $m3 > m1 > m2$. The three colors represent the probability of each mass eigenstate producing a neutrino of each flavor.

The normal hierarchy has a minimum mass of 0.06 eV, whilst the inverted has a minimum mass of 0.1 eV, meaning a measurement of the neutrino mass scale, $M_\nu = \Sigma_i m_i$ of 0.1 eV to a high precision would eliminate the possibility of the inverted hierarchy. We thus have two neutrinos of the same mass $m_1 = m_2$ and the third one of a different mass m_3. We parameterize the masses in terms of the sum of neutrino masses $\sum m_\nu$ and the fraction θ of the total mass in the third neutrino mass eigenstate, so that

$$m_3 = \theta\Sigma m_i. \tag{72}$$

We consider a case where all of the mass is in the third neutrino ($\theta = 1$) or that third neutrino is massless ($\theta = 0$). In the case ($\theta = 1$), we consider $\sum m_\nu = m_3$ and another flavors are zero. The result obtained from analysis of this case is the same of results in above scenario and is close to inverted hierarchy (minimum mass of 0.1 eV). If we consider the case ($\theta = 0$), $\sum m_\nu$ is split to the two equal masses and for each model then, we calculate the minimum mass which is very close to the minimum mass of the normal hierarchy and investigate the effect of non-relativistic neutrino on the structure formation in early universe.

Table 5 χ^2s comparison between ΛCDM and Phantom,Quintessence, and Quintom for the different dataset combinations explored in this work

	CMB + Pantheon+	CMB + BAO	CMB + BAO + Pantheon+
ΛCDM			
$\chi^2_{\rm tot}$	3584.778	2776.072	3593.172
$\chi^2_{\rm CMB}$	2770.254	2769.860	2771.442
$\chi^2_{\rm BAO}$	–	6.212	6.754
$\chi^2_{\rm Pantheon}$	814.524	–	814.976
Phantom			
$\chi^2_{\rm tot}$	3582.5	2768.279	3588.873
$\chi^2_{\rm CMB}$	2769.237	2762.864	2770.013
$\chi^2_{\rm BAO}$	–	5.415	5.752
$\chi^2_{\rm Pantheon}$	813.263	–	813.108
Quintessence			
$\chi^2_{\rm tot}$	3580.152	2766.577	3587.766
$\chi^2_{\rm CMB}$	2766.146	2761.479	2768.365
$\chi^2_{\rm BAO}$	–	5.098	5.176
$\chi^2_{\rm Pantheon}$	814.006	–	814.225
Quintom			
$\chi^2_{\rm tot}$	3580.991	2767.467	3583.151
$\chi^2_{\rm CMB}$	2767.821	2762.113	2769.754
$\chi^2_{\rm BAO}$	–	5.354	5.288
$\chi^2_{\rm Pantheon}$	813.991	–	813.406

The results obtained for the normal hierarchy are:

- For the phantom model (combination data) we obtained $z_{\rm nr} = 113.583$.
- For the quintessence model(combination data) we obtained $z_{\rm nr} = 114.530$.
- For the quintom model (combination data) we obtained $z_{\rm nr} = 112.352$ which is in the matter dominate era. For non-relativistic neutrino wave number.
- For the phantom model (combination data) we obtained the non-relativistic neutrino wave number $k_{\rm nr} = 0.000174{\rm Mp}c^{-1}$.
- For the quintessence model(combination data) we obtained the non-relativistic neutrino wave number $k_{\rm nr} = 0.000175{\rm Mp}c^{-1}$.
- For the quintom model (combination data) we obtained the non-relativistic neutrino wave number $k_{\rm nr} = 0.000173{\rm Mp}c^{-1}$.

Therefore, before and during the radiation era neutrinos are relativistic and behave as radiation, while during and after the matter era neutrinos become non-relativistic and ω_ν becomes 0. Thus, a complete and detailed investigation of the thermal history of the universe requires the exact behavior of $\omega_\nu(z)$, that is its specific form interpolating between these two regimes. Expressing the universe evolution through the redshift z, for convenience, one can have several $\omega_\nu(z)$ parameterizations with the above required properties, namely, the interpolation of the equation of state parameter between $\frac{1}{3}$ to 0. In this work we consider a semi-relativistic phase (around z_{nr}). Following the reference [43], we shall use the following ansatz for $\omega_\nu(z)$

$$\omega_\nu(z) = \frac{p_\nu}{\rho_\nu} = \left(1 + tanh\left(\frac{ln(1+z) - z_{\rm eq}}{z_{\rm dur}}\right)\right) \tag{73}$$

where $z_{\rm eq}$ determines the transition redshift where matter and radiation energy densities become equal and $z_{\rm dur}$ determines how fast this transition is realized. In summary, using the dimensionless variable ω_ν, we can transform Eq. (70) into its autonomous form:

$$\frac{d\omega_\nu}{dN} = \frac{2\omega_\nu}{z_{\rm dur}}(3\omega_\nu - 1). \tag{74}$$

In order to put observational constrain on parameter $\omega_{\nu 0}$ and reconstruct the evolution of ω_ν, the above equation should be coupled to the autonomous equations of the three models. By doing this, we have reconstructed the evolution of ω_ν using observational constraint. In Fig. 12, we depicted the evolution of ω_ν for three models. As can be seen, neutrino equation of state parameter ($\omega_\nu(z)$) evolve from radiation dominated with value of $\omega_\nu = \frac{1}{3}$.

Moreover, we desire to have a better control on the features of this transition, namely, the epoch around which the

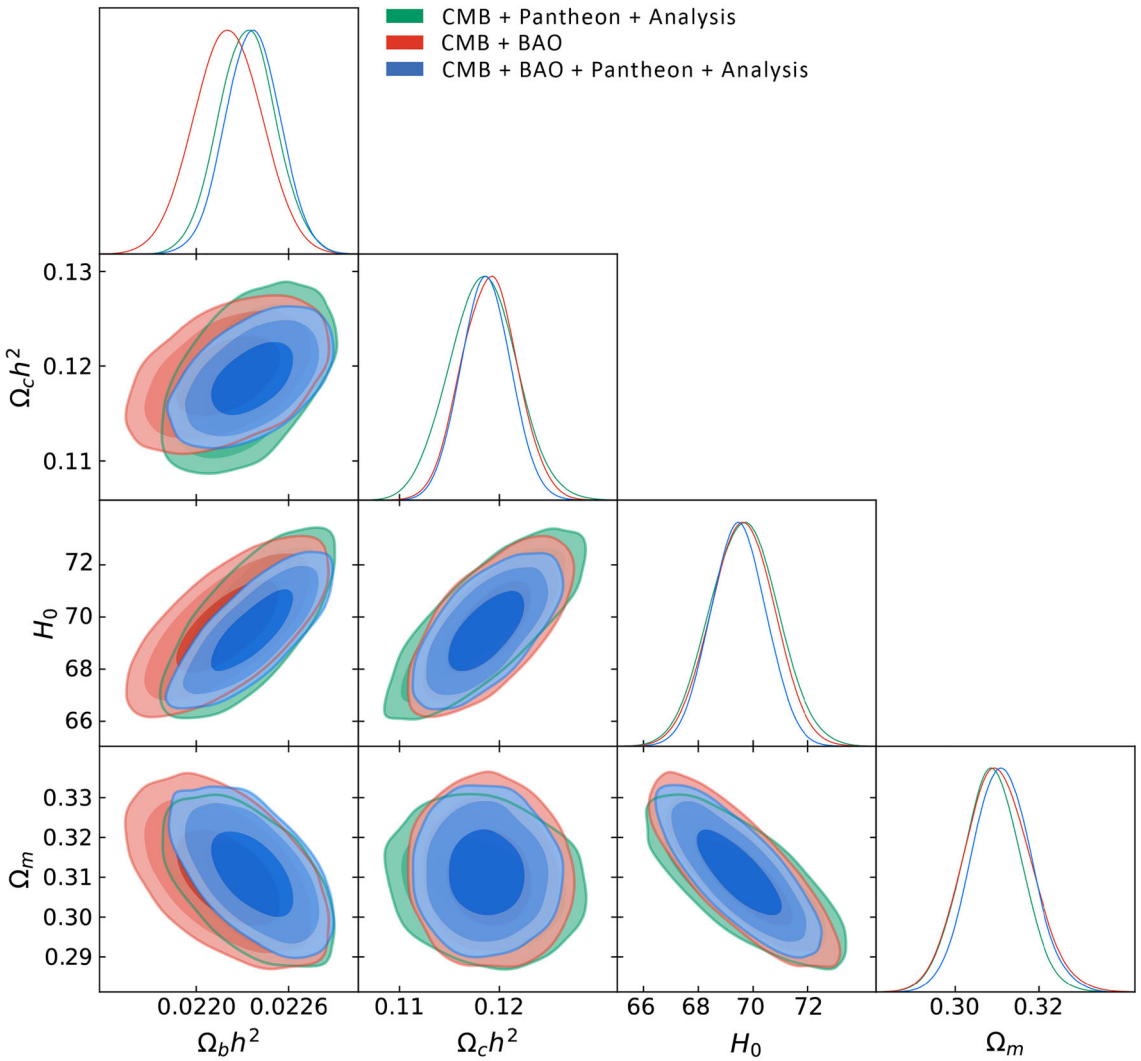

Fig. 7 Comparison of $\Omega_b h^2$, $\Omega_c h^2$, H_0, Ω_m obtained values in phantom model

transition is realized and the duration of realization. We consider a semi-relativistic phase (around z_{nr}) between relativistic to non-relativistic transition, where the neutrino equation of state parameter ($\omega_\nu(z)$) varies from 0 to $\frac{1}{3}$. To avoid rewriting the equations of each scalar field, we only show the results of our analysis in Fig. 12. By doing this we obtained that during the radiation dominated era $\omega_\nu = \frac{1}{3}$ and in the recent universe ($\omega_\nu = 0.012$, $z_{dur} = 3.61$), ($\omega_\nu = 0.014$, $z_{dur} = 3.63$) and $\omega_\nu = 0.026$, $z_{dur} = 3.88$ for quintessence model, Phantom and Quintom model respectively (Fig. 13). The results are in good agreement with the results of [43].

4 Conclusion

The addition of massive neutrinos to the cosmological model alters both the redshift evolution of $H(z)$, and the clustering of matter on small scales. By combining different cosmological observables sensitive to these effects, it is forecasted that data from upcoming surveys have the potential to reach the precision required to make the first observational detection of neutrino mass [19].

In this paper, we used phantom, quintessence and quintom as dark energy and put a constraint on neutrino mass by coupling dark energy with neutrino. We first found that the total mass of neutrino is $\sum m_\nu < 0.1197eV$ (95% confidence level (C.L.) for quintom model and $\sum m_\nu <$ 0.121eV(95% confidence level (C.L.) for phantom model and $\sum m_\nu <$ 0.122eV (95% confidence level (C.L.) for quintessence model. These results are in broad agreement with the results of Planck 2018 where the limit of the total neutrino mass is $\sum m_\nu <$ 0.12eV (95% C.L., TT, TE, EE+lowE+lensing+BAO). Also, the interaction constant, β, for these three models are investigated.

As we know, larger β will generally lead to larger m_ν in the universe.

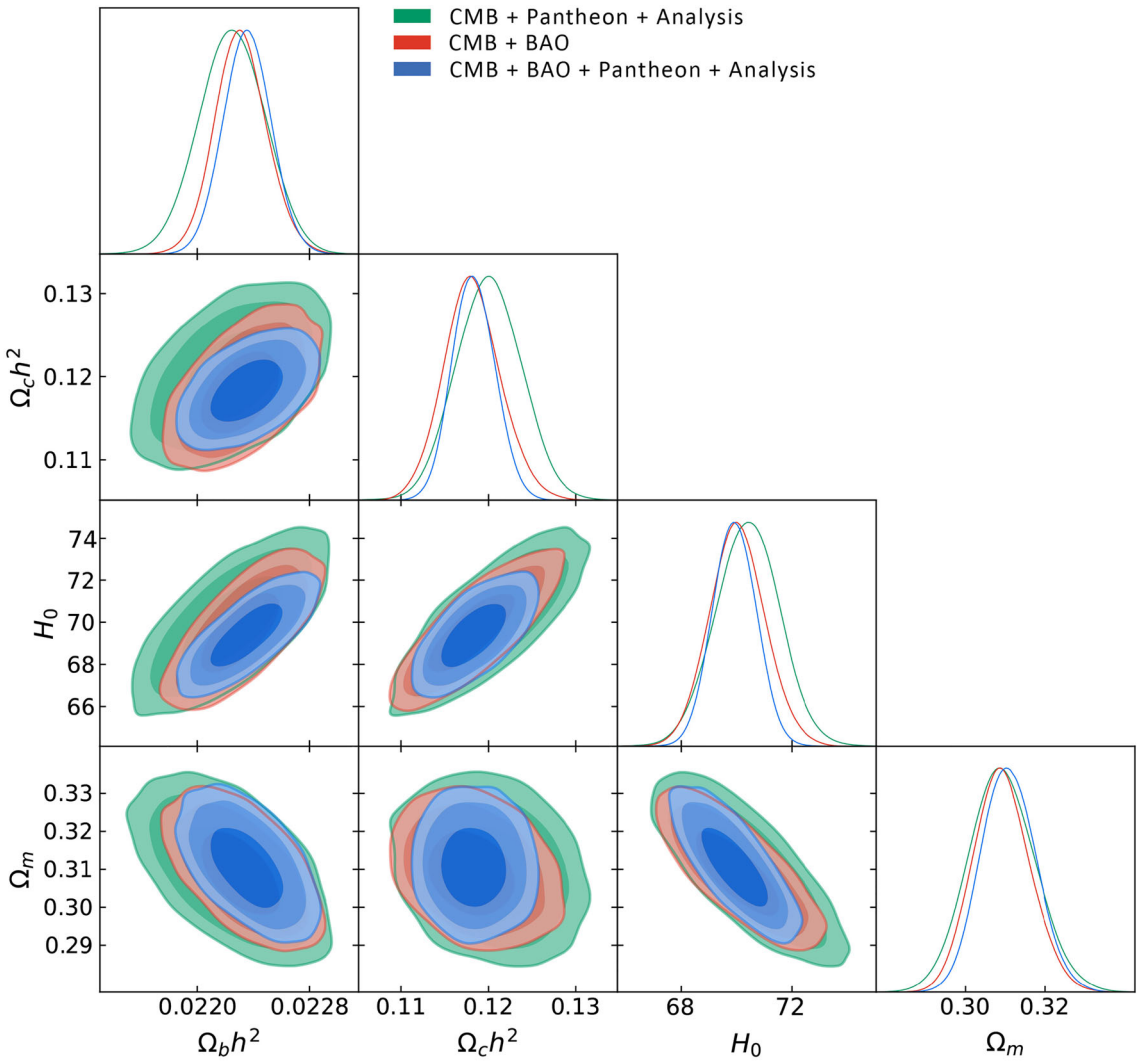

Fig. 8 Comparison of $\Omega_b h^2$, $\Omega_c h^2$, H_0, Ω_m obtained values in quintessence model

- In phantom model, the value of β for combination data (Pantheon + CMB + BAO) is 0.229. This value indicate that the coupling between neutrino and dark energy is small.
- In quintessence model, β is 0.63 which indicates that the dark energy neutrino interaction is grater than that of phantom model.
- β value in the quintum model is about 0.236, which shows that in the world of quintom, the coupling between neutrino and dark energy almost is the same as what phantom model has predicted. What is more, the results obtained in this paper indicate that the value of the equation of state in the quintom model is $\omega_\sigma = -1.04 \quad \omega_\phi = -1$. By comparing the results obtained for the equation of state of these three models, it can be concluded that for the equation of state with a value of -1 or less (Quintom and Phantom models), the value of dark energy neutrino interaction is less than a situation when the equation of state value is greater than -1 (Quintessence model). In what follows, we surveyed $z_{\rm nr}$ for all three models and we obtained:
- For the phantom model(combination data) we obtained $z_{\rm nr} = 228.166$
- For the quintessence model(combination data) we obtained $z_{\rm nr} = 230.060$
- For the quintom model(combination data) we obtained $z_{\rm nr} = 225.704$

these results shows that the neutrinos become non-relativistic at distance almost 4282Mpc or 13.7Gly Although this amount is much less than $z_{\rm eq}$.

Also, we indicated that the non-relativistic neutrino plays an important role in structure formation at the early universe. The results obtained in this paper for co-moving wavenumber ($k_{\rm nr} \approx 0.018\Omega_m{}^{\frac{1}{2}}(\frac{m_\nu}{1ev})^{\frac{1}{2}} h{\rm Mpc}^{-1}$) are:

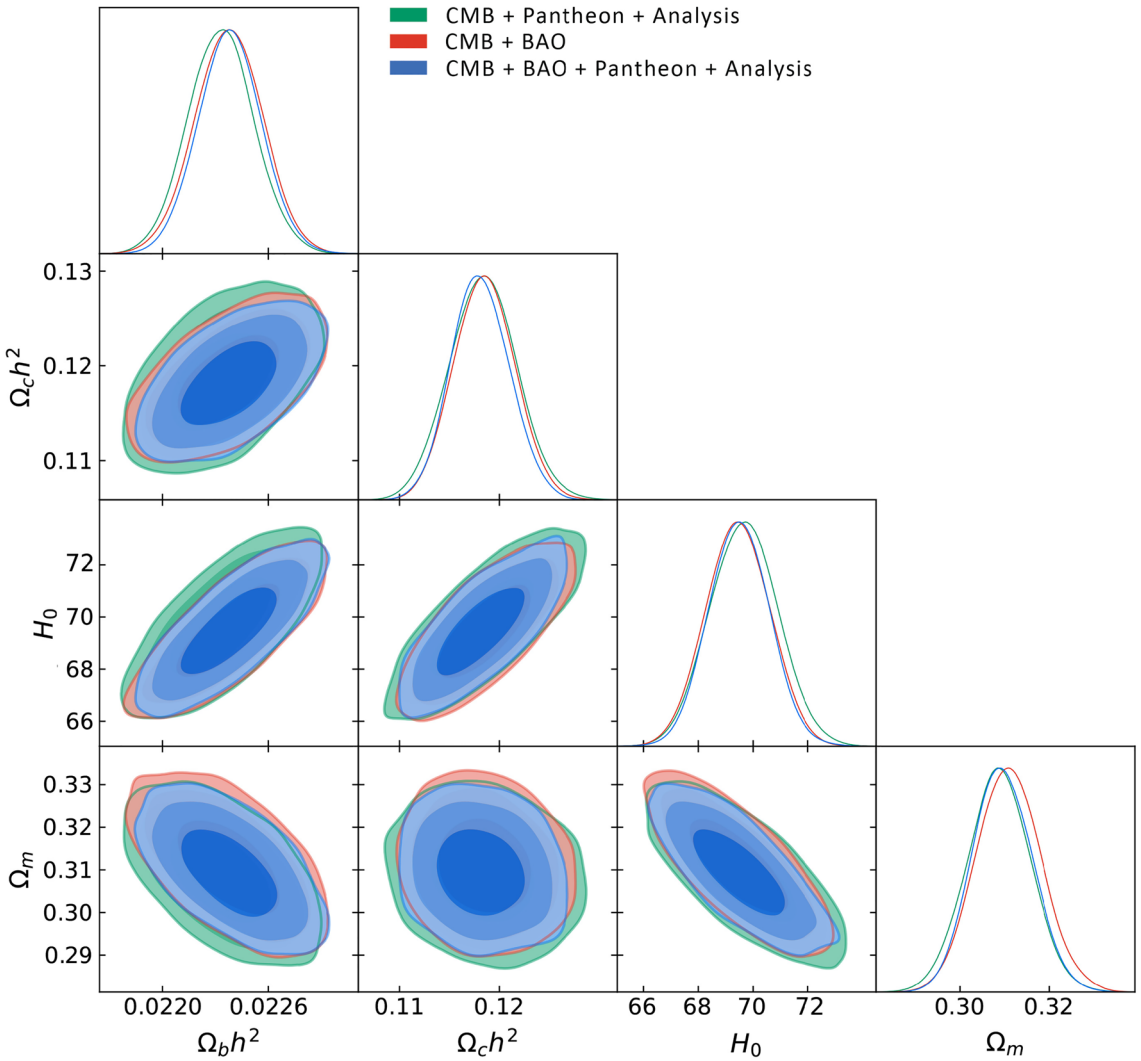

Fig. 9 Comparison of $\Omega_b h^2$, $\Omega_c h^2$, H_0, Ω_m obtained values in quintom model

- For the phantom model(combination data) we obtained the non-relativistic neutrino wavenumber $k_{nr} = 0.0.000243 \text{Mpc}^{-1}$.
- For the quintessence model(combination data) we obtained the non-relativistic neutrino wavenumber $k_{nr} = 0.000248 \text{Mpc}^{-1}$.
- For the quintom model(combination data) we obtained the non-relativistic neutrino wavenumber $k_{nr} = 0.000245 \text{Mpc}^{-1}$. These results are in general agreement with [15,27]. these results are in good agreement [15,27]. Furthermore, we consider the scenario when $\sum m_\nu$ equals to the minimum value in each hierarchy and the lightest neutrino is massless. We work on the case that all of the mass is in the third neutrino ($\theta = 1$) or that third neutrino is massless ($\theta = 0$). In the case ($\theta = 1$), we consider $\sum m_\nu = m_3$ and another flavors are zero. Results were obtained from analysis of this case is the same of results in above scenario and is close to inverted hierarchy (minimum mass of 0.1 eV). If we consider the case ($\theta = 0$), $\sum m_\nu$ split to the two equal mass and for each model we calculate the minimum mass which is very close to the minimum mass of the normal hierarchy. The results obtained for the normal hierarchy are:
- For the phantom model(combination data) we obtained $z_{nr} = 113.583$.
- For the quintessence model(combination data) we obtained $z_{nr} = 114.530$.
- For the quintom model(combination data) we obtained $z_{nr} = 112.352$ which is in the matter dominate era. For non-relativistic neutrino wave number.
- For the phantom model(combination data) we obtained the non-relativistic neutrino wave number $k_{nr} = 0.000174 \text{Mpc}^{-1}$.
- For the quintessence model(combination data) we obtained the non-relativistic neutrino wave number $k_{nr} = 0.000175 \text{Mpc}^{-1}$.

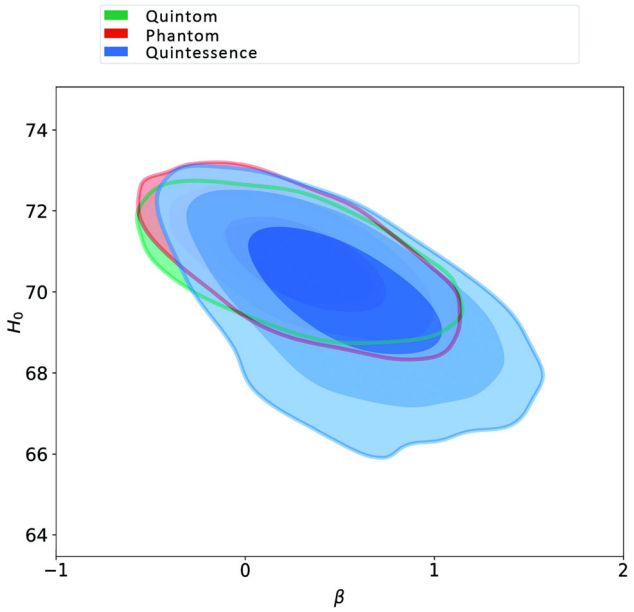

Fig. 10 Comparison of β value obtained for combined data (CMB + BAO + Pantheon) in three models

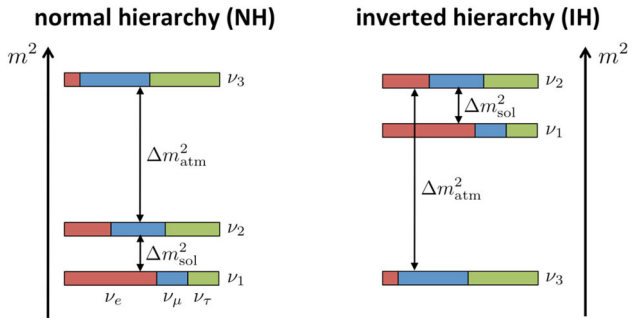

Fig. 11 The results of oscillation experiments lead to two possible orderings of the neutrino mass eigenstates

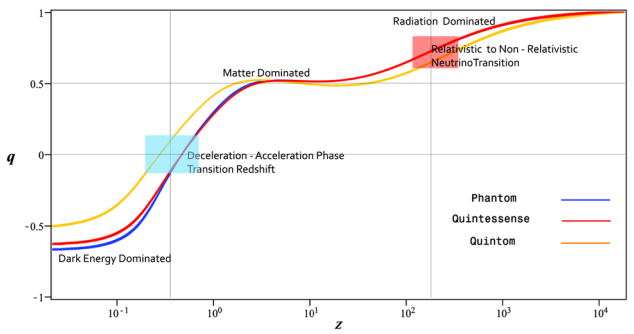

Fig. 12 The plots show the evolution of of deceleration parameter q as a function of the redshift for the best-fitted values of the parameters in all three model

- For the quintom model(combination data) we obtained the non-relativistic neutrino wave number $k_{\rm nr} = 0.000173 {\rm Mp}c^{-1}$.

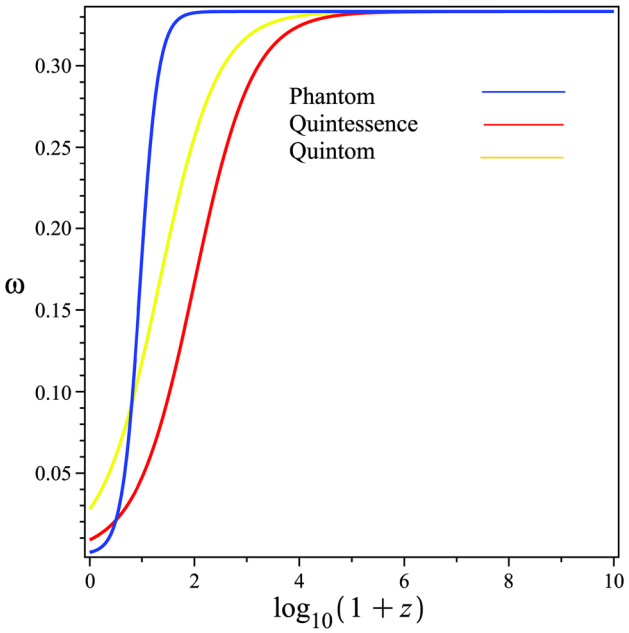

Fig. 13 Figure shows the evolutions of equation of state parameters ω_ν for all three models

Also, we consider a semi-relativistic phase (around $z_{\rm nr}$) between relativistic to non-relativistic transition and we find that during the radiation dominated era $\omega_\nu = \frac{1}{3}$ and in the recent Universe ($\omega_\nu = 0.012, z_{\rm dur} = 3.61$) for the quintessense model; ($\omega_\nu = 0.014, z_{\rm dur} = 3.63$) for the phantom model; $\omega_\nu = 0.026, z_{\rm dur} = 3.88$ for the quintom model which is consistent with results of the study carried out by [43].

Moreover, we obtain the Δ(AIC) Between ΛCDM and each model.

- The value of Δ(AIC) between the phantom model and ΛCDM is 0.299.
- The value of Δ(AIC) between the Quintessence model and ΛCDM is 1.406.
- The value of Δ(AIC) between the Quintom model and ΛCDM is 6.021.

As we can see in Table 4, the analyses based on the AIC indicated that there is more support for the interacting scalar fields with the neutrinos when compared to the ΛCDM model, and fit better than ΛCDM for the full dataset combination, and improving the χ^2.

Data availability This manuscript has no associated data or the data will not be deposited. [Authors' comment: Data is available upon request from Authors.]

Funded by SCOAP[3]. SCOAP[3] supports the goals of the International Year of Basic Sciences for Sustainable Development.

References

1. P.A.R. Ade et al. Planck Collaboration, A&A **A13** (2016)
2. N. Aghanim et al. Planck Collaboration, arXiv:1907.12875
3. Q.R. Ahmad et al., Phys. Rev. L **87**(7), 071301 (2001)
4. S. Alam et al., MNRAS **470**, 2617 (2017)
5. L. Amendola, Phys. Rev. D **62**, 043511 (2000)
6. C. Armendariz-Picon, V. Mukhanov, P.J. Steinhardt, Phys. Rev. Lett. **85**, 4438 (2000)
7. M. Baldi, MNRAS **411**, 1077 (2011)
8. R. Bean, E.E. Flanagan, M. Trodden, Phys. Rev. D **78**, 023009 (2008)
9. F. Beutler, C. Blake, M. Colless et al., MNRAS **416**, 3017 (2011)
10. N. Bilic, G.B. Tupper, R.D. Viollier, Phys. Lett. B **535**, 17 (2002)
11. A.W. Brookfield, C. van de Bruck, D.F. Mota, D. Tocchini-Valentini, Phys. Rev. D **73**, 083515 (2007)
12. Caldwell et al. (2003). arXiv:astro-ph/0302506v1
13. S.M. Carroll, Living Rev. Relativ. **4**, 1 (2001)
14. T. Chiba, T. Okabe, M. Yamaguchi, Phys. Rev. D **62**, 023511 (2000)
15. G. Christos, Eur. Phys. J. C **81**, 753 (2021)
16. E.J. Copeland, M. Sami, S. Tsujikawa, Int. J. Mod. Phys. D **15**, 1753 (2006)
17. R. Davis, Prog. Part. Nucl. Phys. **32**, 1332 (1994)
18. G.R. Farrar, P.J.E. Peebles, ApJ **604**, 1 (2004)
19. A. Font-Ribera et al., J. Cosmol. Astro-Part. Phys. **023**, 023 (2014)
20. Y. Fukuda et al., Phys. Rev. L **81**(8), 15621567 (1998)
21. A. Gelman, D.B. Rubin, Stat. Sci. **1992**(7), 457–472 (1992)
22. Z.K. Guo, Y.S. Piao, X.M. Zhang, Y.Z. Zhang, Phys. Lett. B **608**, 177 (2005)
23. T. Kajita, Nucl. Phys. B Proc. Suppl. **77**(1–3), 123132 (1999) [hep-ex] (cit. on p. 38)
24. J. Lesgourgues, P. Sergio, Phys. Rep. **429**, 307379 (2006)
25. A. Lewis, S. Bridle, Phys. Rev. D **2002**(66), 103511 (2002)
26. A. Lewis, Phys. Rev. D **2013**(87), 103529 (2010)
27. M. Shoji, E. Komatsu, Phys. Rev. D **81**, 123516 (2010)
28. S. Nojiri, S.D. Odintsov, Phys. Rep. **505**, 59 (2011)
29. K. Nozari, N. Rashidi, Adv. High Energy Phys. **2013**, 803735 (2013)
30. K. Nozari, M.R. Setare, T. Azizi, N. Behrouz, Phys. Scr. **80**, 025901 (2009)
31. T. Padmanabhan, Phys. Rep. **380**, 235 (2003)
32. P.J.E. Peebles, B. Ratra, Astrophys. J. **325**, L17 (1988)
33. S. Perlmutter et al., Astrophys. J. **517**, 565 (1999)
34. V. Pettorino, C. Baccigalupi, Phys. Rev. D **77**, 103003 (2008)
35. B. Ratra, P.J.E. Peebles, Phys. Rev. D **37**, 3406 (1988)
36. A.G. Riess et al., Astron. J. **116**, 1009 (1998)
37. A.J. Ross, L. Samushia, C. Howlett et al., MNRAS **449**, 835 (2015)
38. V. Sahni, A. Starobinsky, Int. J. Mod. Phys. D **9**, 373 (2000)
39. A. Salehi et al., MNRAS/stab909 (2021)
40. A. Sen, JHEP **0207**, 065 (2002)
41. T.P. Sotiriou, V. Faraoni, Rev. Mod. Phys. **82**, 451 (2010)
42. D. Scolnic et al., ApJ **938**(2) (2022)
43. W. Hossain, M. Myrzakulov, R. Sami, M. Saridakis, E. N., Phys. Rev. D **90**, 023512 (2014)
44. C. Wetterich, Astron. Astrophys. **301**, 321 (1995)
45. C. Wetterich, Nucl. Phys. B **302**, 668 (1988)
46. M.M. Zhao, J.F. Zhang, X. Zhang, Phys. Lett. B **779**, 473 (2018)
47. X.F. Zhang, H. Li, Y.S. Piao, X.M. Zhang, Mod. Phys. Lett. A **21**, 231 (2006)
48. I. Zlatev, L.M. Wang, P.J. Steinhardt, Phys. Rev. Lett. **82**, 896 (1999)